

## Nearly straight line trajectories of the standard map with twist

This article has been downloaded from IOPscience. Please scroll down to see the full text article.

1991 J. Phys. A: Math. Gen. 24 3455

(<http://iopscience.iop.org/0305-4470/24/15/017>)

View [the table of contents for this issue](#), or go to the [journal homepage](#) for more

Download details:

IP Address: 129.252.86.83

The article was downloaded on 01/06/2010 at 11:09

Please note that [terms and conditions apply](#).

## Nearly straight line trajectories of the standard map with twist

P H Borchers<sup>†</sup> and G P McCauley<sup>‡</sup>

<sup>†</sup> School of Physics and Space Research, University of Birmingham, Birmingham B15 2TT, UK

<sup>‡</sup> School of Mathematics and Statistics, University of Birmingham, Birmingham B15 2TT, UK

Received 21 January 1991

**Abstract.** Some trajectories of the standard map with twist appear to be 'nearly straight lines'. In order to understand the cause of this appearance, a two-dimensional Hamiltonian function with rotational symmetry derived from the map has been studied. For three-, four- or six-fold symmetry, the plane is tiled periodically by sets of parallel straight line energy contours joining the hyperbolic fixed points. For other rotational symmetries, periodic tiling of the plane is not possible, but in some cases there is a strong appearance of quasi-periodic tiling by energy contours, corresponding to nearly straight line trajectories of the map. Such energy contours are associated with straight lines along which the variance of the Hamiltonian is a local minimum. For five- and eight-fold symmetry the local minimum value of the variance along such lines decreases quadratically with perpendicular distance from the origin. For seven-fold symmetry, it appears to vary approximately inversely with distance from the origin. With these rotations, energy contours can be found which are as close to straight lines as we please and which correspond to nearly straight line trajectories of the standard map with twist.

### 1. Introduction

The mapping  $M_q$  defined by

$$x_{n+1} = (x_n + k \sin y_n) \cos(2\pi/q) + y_n \sin(2\pi/q) \quad (1a)$$

$$y_{n+1} = -(x_n + k \sin y_n) \sin(2\pi/q) + y_n \cos(2\pi/q) \quad (1b)$$

is known as the standard map with twist (Sagdeev *et al* 1988),  $k$  is called the nonlinear parameter. The properties of this mapping are most interesting near resonance, i.e. when the rotation number  $q$  is an integer.

In the limit of small values of  $k$ , the  $q$ th iteration of the mapping, i.e.  $(M_q)^q$ , is approximately the identity. The mapping  $M_q$  generates  $q$  symmetrically related images, which are traversed at a rate proportional to  $k$ . These sets of points are known as the phase trajectories of the map.

If the rotation number  $q$  is 'crystallographic' ( $q = 3, 4$  or  $6$ ), and the parameter  $k$  is not too large, then orbits of this mapping generate points that lie close to the lines of a periodic tiling of the plane.

The smaller the value of  $k$ , the more nearly do certain trajectories tile the plane; in the limit  $k \rightarrow 0$  the tiling is truly periodic. This tiling is manifested by straight line trajectories which divide the plane into squares ( $q = 4$ ) or into a pattern of triangles and hexagons (cf figure 1) ( $q = 3$  and  $q = 6$ ).

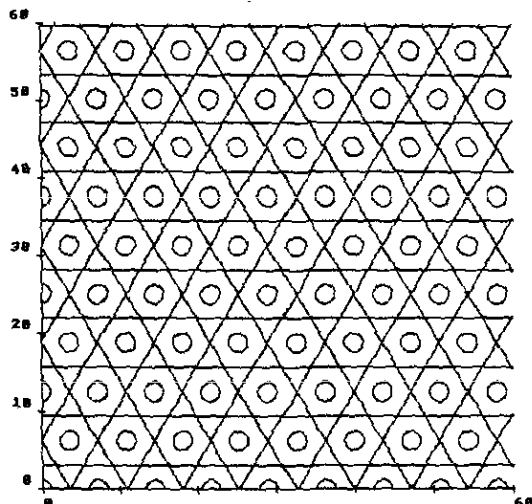


Figure 1. Energy contours of the function  $\mathcal{H}_3$  at Hamiltonian values  $-1$  and  $+2$ . The energy contour at  $-1$  consists of straight lines connecting the saddle points and forms a periodic net tiling the plane. (The energy contours of  $\mathcal{H}_6$  are similar: multiply the values of the Hamiltonian  $\mathcal{H}_3$  by 2.)

For all values of the rotation number  $q$  other than the crystallographic values it is well known that periodic tiling of the plane is not possible. However even for non-crystallographic values of  $q$ , the mapping  $M_q$  does generate some trajectories which appear to be *very nearly straight lines* (see Chernikov *et al* 1987a and cf figures 3-6 of this paper). As  $k$  decreases the 'nearly straight line' trajectories become better and better defined, but even in the limit  $k=0$  they are not straight lines.

For large values of  $k$  the mapping no longer generates well-defined trajectories: as  $k$  increases the trajectories develop into a stochastic web (Chernikov *et al* 1987a). We are here restricting attention to small values of  $k$ , indeed to what happens when  $k=0$ , and shall not further discuss what happens for large values of  $k$ .

Direct examination of the trajectories of the mapping, while yielding attractive displays on the monitor of a microcomputer, did not yield much insight into why some trajectories in the non-crystallographic cases appeared to be almost straight lines. Such a direct examination was unhelpful in solving this problem, and was also very time consuming for small values of  $k$ .

As shown in appendix A phase trajectories of the mapping  $(M_q)^q$  correspond to energy contours of the Hamiltonian function:

$$\mathcal{H}_q(x, y) = \sum_{p=0}^{q-1} \cos\{y \cos(2\pi p/q) - x \sin(2\pi p/q)\}. \quad (2)$$

The period  $q$  points of the mapping  $M_q$  correspond to the stationary points of this Hamiltonian function; extrema of the Hamiltonian correspond to elliptic points, and saddle points to hyperbolic points. In this paper we shall be particularly concerned with hyperbolic fixed points and the associated trajectories and contours.

A hyperbolic point has (usually) two incoming and two outgoing trajectories. These trajectories separate the plane into unconnected regions and are called separatrices: they correspond to energy contours through saddle points.

A merit of studying the Hamiltonian (equation (2)) rather than the mapping (equation (1)) in the limit of small nonlinearity is that the time to complete a typical orbit of the mapping is inversely proportional to the magnitude of the nonlinear parameter  $k$ . This is compounded by the extremely long time taken to complete an orbit close to a separatrix. (To complete a separatrix orbit takes an infinite time: the rate at which a hyperbolic fixed point is approached is vanishingly small.) Plotting a contour is not affected by the rate at which the corresponding trajectory is generated.

## 2. Tiling of the plane

Figures 1 and 2 show energy contours of  $\mathcal{H}_3$  and  $\mathcal{H}_4$  passing through saddle points. The plane is tiled periodically by these straight lines, which are separatrices of the mappings  $M_3$  and  $M_4$  in the limit  $k \rightarrow 0$ .

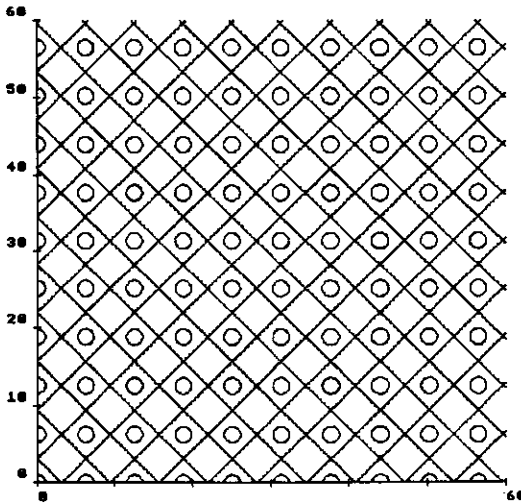


Figure 2. Energy contours of  $\mathcal{H}_4$  at 0 and +3. The energy contour at 0 consists of straight lines connecting the saddle points, and forms a periodic net tiling the plane.

A periodic tiling of the plane can have two-, three-, four- or six-fold symmetry: we refer to these as crystallographic symmetries. When  $q$  has any other (integer) value, a periodic tiling of the plane is not possible. However if we examine the energy contours of  $\mathcal{H}_5$ ,  $\mathcal{H}_7$  or  $\mathcal{H}_8$  (figures 3–6) we find many centres of approximate local symmetry reminiscent of quasiperiodic tilings.

Chernikov *et al* (1987a) have remarked on the similarity between the mapping with twist and the structure of so-called ‘quasicrystals’. There have been reports of materials appearing to display five-fold ‘crystalline’ symmetry (Schechtman *et al* 1984). The quasiperiodic tilings are two-dimensional cuts of higher dimensional periodic functions (Bak 1985).

In a crystallographic case, when the Hamiltonian has three-, four- or six-fold symmetry the saddle points are related by symmetry and all have the same energy: the net of separatrices is continuous and the separatrices are infinitely long straight lines.

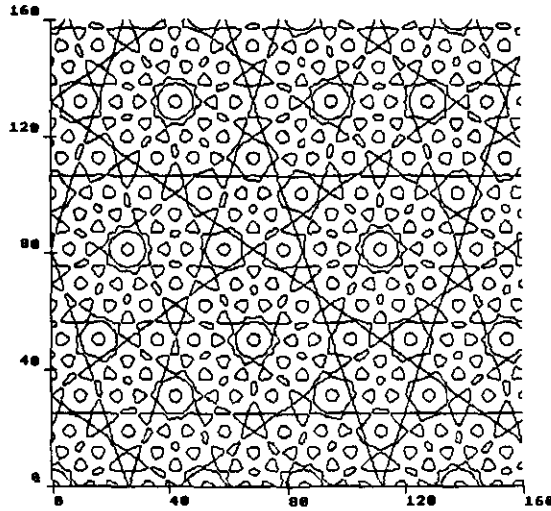


Figure 3. Energy contours of  $\mathcal{H}_5$  at Hamiltonian 0.96. Note that all the curves lie at a single value, which is close to the peak value in the density of states. It can be seen that some of the contours appear to 'almost lie on a straight line', e.g. the line near  $y = 106$ , and the other lines at the same distance from the origin: along these lines the variance of the Hamiltonian is  $2.8 \times 10^{-4}$ .

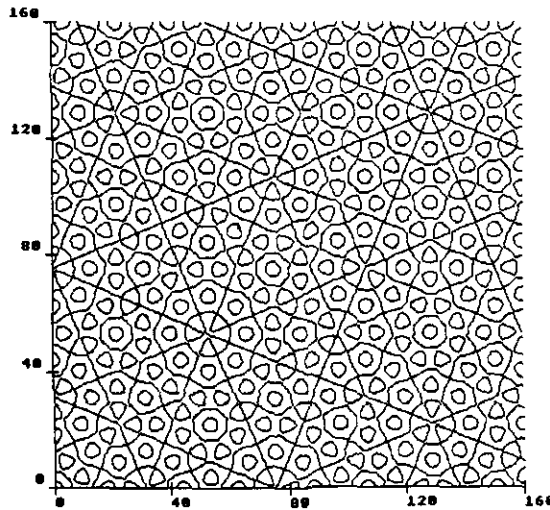


Figure 4. Energy contours of  $\mathcal{H}_8$  at a Hamiltonian value 0. As in figures 3, all the curves lie at a single value, close to the peak in the density of states. Again, certain contours appear to 'lie almost on a straight line'. In the figure there are three sets of lines each a factor of 2.414... farther from the origin, on which the variance of the Hamiltonian is particularly small (see table 2).

In the non-crystallographic cases (all other values of  $q$ ), there is no symmetry relating all the saddle points: the value of the energy at saddle points is distributed over a range (as can be shown by density of states calculations, Chernikov *et al* 1987b). There is no continuous net of separatrices joining all the hyperbolic fixed points, and the separatrices are *not* straight lines.

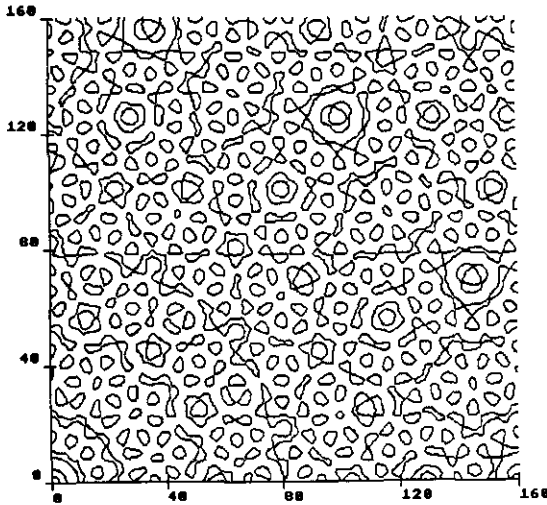


Figure 5. Energy contours of  $\mathcal{H}_7$  at a Hamiltonian value  $-0.99$ , close to the peak in the density of states. In comparison with figures 3 and 4, the apparent 'straight lines' are less marked.

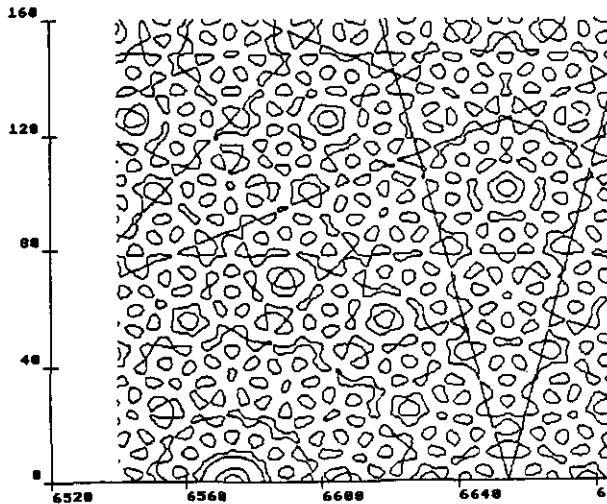


Figure 6. Energy contours of  $\mathcal{H}_7$  at a Hamiltonian value  $-0.99$ , close to the peak in the density of states. In comparison with figure 5, the pair of intersecting 'quasi straight line' contours passing through the point  $(6650, 0)$  is considerably more evident. Along these lines the variance of the Hamiltonian is  $9.21 \times 10^{-4}$  (see table 3).

It has been suggested (Chernikov *et al* 1987a) that the separatrices of  $M_5$  are fractal: it is true that there is some degree of self-similarity over a range of scales, but there is a minimum scale length (of a few units) corresponding to the spacing of the saddle points: at distances less than this, the structure of the phase trajectories (energy contours) is smooth and uninteresting.

To study the patterns produced by the non-crystallographic mappings  $M_5$ ,  $M_7$  and  $M_8$  we have investigated the *variance* of the corresponding Hamiltonian function along straight lines in the plane.

It is straightforward to derive analytic expressions for the variance  $v_q$  of the Hamiltonian  $\mathcal{H}_q$  along an infinitely long straight line: along a general line the variance is constant (and equal to  $q$  or to  $q/2$ , depending upon whether  $q$  is even or odd); however, along lines making an angle which is a multiple of  $\pi/q$  to the  $x$ -axis, the variance depends strongly (and quasiperiodically) on the distance of such a line from the origin.

In the crystallographic cases the minimum variance along such a special straight line can be zero: the lines are energy contours, as we already know.

In the non-crystallographic cases, the variance along a straight line can never actually be zero, but in certain cases it is possible to find lines along which the variance is as small as we please.

In the three cases,  $q = 5, 7$  and  $8$ , it is easy to find lines along which the variance is small, as can be seen in figures 3-6. Indeed for  $q = 5$  and  $q = 8$ , as we shall see in the next sections, there are analytic results showing that successive least minima of the variance fall off inversely with the square of the distance of the line from the origin. For  $q = 7$ , successive least minima of the variance appear to fall off more slowly with distance, perhaps linearly, but the relation appears to be 'stochastic' (see figure 7).

When the rotational symmetry  $q$  has a value greater than those discussed here, the least value of the variance along a straight line does not appear to approach zero.

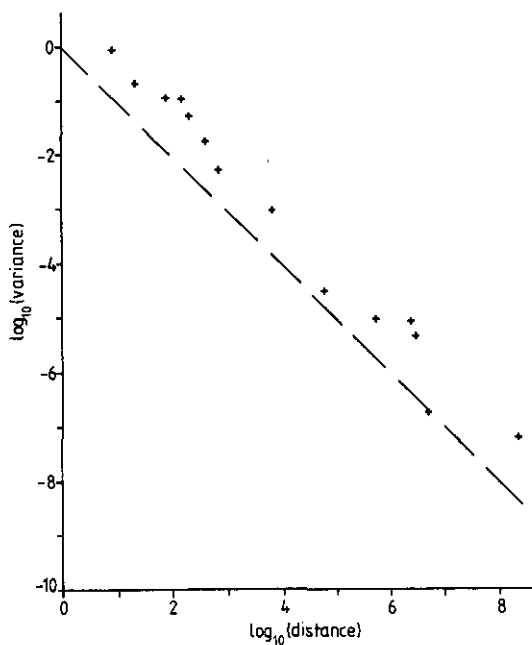


Figure 7. Logarithmic plot showing successive least minima in the variance of  $\mathcal{H}_7$  along straight lines plotted against the distance of the line from the origin.

### 3. Minimal variance of $\mathcal{H}_q$

The variance of  $\mathcal{H}_q$  along a general line in the plane is constant, but along certain symmetry related lines, the variance depends upon the distance of those lines from

the origin. It is necessary to distinguish three types of behaviour, depending upon the value of  $q$ .

(a)  $q$  odd. The minima lie on lines parallel to the  $x$ -axis (and along lines at an angle which is a multiple of  $\pi/q$  to the  $x$ -axis).

(b)  $q = (4n+2)$ . In this case, the Hamiltonian is just double that for  $q = 2n+1$ , i.e.  $\mathcal{H}_{4n+2} = 2\mathcal{H}_{2n+1}$ .

(c)  $q = 4n$ . The minima lie on lines which make an angle equal to an odd multiple of  $\pi/q$  to the  $x$ -axis.

When the distance from the origin of a line with appropriate slope is an odd multiple of  $\pi$  (independent of the value of  $q$ ), the variance of the Hamiltonian along it is a maximum.

#### 4. Five-fold symmetry

The variance of the Hamiltonian  $\mathcal{H}_5$  along the line  $y = d$  is given by

$$\begin{aligned} v_5(d) &= 2 + \frac{1}{2} \sum_{p=1}^4 \cos(2d \cos(2\pi p/5)) \\ &= 2 + \cos(d/\phi) + \cos(d(1+1/\phi)) \end{aligned} \quad (3)$$

where  $\phi = (1 + \sqrt{5})/2 = 1.618 \dots$ , the golden ratio.

When  $d$  is a multiple of  $\pi$ , equation (3) simplifies to

$$v_5(n\pi) = 2 + (1 + (-1)^n) \cos(n\pi/\phi). \quad (4)$$

When  $n$  is odd, the variance is equal to 2, exactly. When  $n$  is even

$$v_5(2n\pi) = 2(1 + \cos(2n\pi/\phi)) \quad (5)$$

and this will be small if  $(2n\pi/\phi)$  is approximately equal to an odd multiple of  $\pi$ , say,  $(2k+1)\pi$ . Thus we expect to find small minima when we have good integer approximations to the value of  $\phi$ , in the form  $2n/(2k+1)$ .

It is a well known result in number theory (Hardy and Wright, 1954) that the best rational approximations (convergents) to any number are obtained from its continued fraction expansion. The convergents to  $\phi$  are given by the ratio of successive terms of the Fibonacci series. The requirement that the numerator be even limits us to every third term in the Fibonacci series. The agreement between our prediction and observation is shown in table 1. From the general theory of continued fractions it is known also that the difference between a quantity and its convergent is less than the square

Table 1. Successive least minima of  $v_5$ .

Distance	Variance	Distance/ $\pi$	Distance/ $\pi\phi$	Fibonacci numbers	(Variance) $\times$ (distance) <sup>2</sup>
5.7323	0.091	1.82	1.12	[2, 1]	2.97
25.263	5.1 E-3	8.04	4.97	[8, 5]	3.25
106.78	2.8 E-4	33.99	21.01	[34, 21]	3.24
452.40	1.6 E-5	144.00	89.00	[144, 89]	3.22
1916.4	8.8 E-7	610.00	377.00	[609, 377]	3.23



of the denominator of the rational fraction. Applying this we find that the variance should fall off with the square of the distance of the line from the origin. This is indeed observed, as can be seen from the final column of table 1.

Each successive 'least minimum' occurs on a line which is approximately  $\phi^3$  farther from the origin than its predecessor, while the value of the variance falls by a factor  $\phi^6$  at each step. Thus we can predict where to look for a line on which the variance is arbitrarily small.

### 5. Eight-fold symmetry

The variance of the Hamiltonian  $\mathcal{H}_8$  along a line lying at an angle  $\pi/8$  to the  $x$  axis, and a distance  $d$  from the origin is given by

$$v_8(d) = 8 + 4[\cos\{d\sqrt{2+\sqrt{2}}\} + \cos\{d\sqrt{2-\sqrt{2}}\}]. \quad (6)$$

The condition for a minimum is that the arguments of each of the cosines be close to an odd multiple of  $\pi$ . This can be shown to be equivalent to finding rational convergents to  $(\sqrt{2}+1)$ . As in the case of five-fold symmetry, the least variance falls off quadratically with distance, although at a given distance, the absolute value of the least minimum is greater for  $v_8$  than for  $v_5$ , as can be seen by comparing the final columns of tables 1 and 2.

Table 2. Successive least minima of  $v_8$ .

Distance	Variance	(Variance) $\times$ (Distance) <sup>2</sup>
11.951	0.170	24.305
28.883	0.029	24.466
69.718	5.03 E-3	24.476
168.32	8.63 E-4	24.397
406.35	1.48 E-4	24.480
981.025	2.54 E-5	24.489

Each successive least minimum occurs approximately  $(1+\sqrt{2})$  times farther from the origin than the previous one.

In each of the five- and eight-fold symmetries, the condition for a minimum variance depends upon two irrational quantities being simultaneously approximated by a rotational fraction as seen in equations (3) and (6). In both cases this requirement can be further simplified (using trigonometric identities) to finding a good rational approximation for a single irrational number. It is this simplification that leads to the quadratic rate of fall in the variance. Moreover in both cases the irrational number in question is the root of a quadratic, so the successive denominators satisfy a linear two-term recurrence relation. Hence the successive least minima occur regularly.

This does not pertain for any other symmetry, so it is unlikely that a similar dependence of least successive variance on distance will be found at any higher values of  $q$ .

## 6. Seven-fold symmetry

The variance of the Hamiltonian  $\mathcal{H}_7$  along the line  $y = d$  is

$$v_7(d) = 3 + \sum_{p=1}^3 \cos(2d \cos(p\pi/7)). \quad (7)$$

In contrast to the previous cases, it is now necessary to find rational approximations, all with the same denominator, to the three irrational quantities,  $\cos(\pi/7)$ ,  $\cos(2\pi/7)$  and  $\cos(3\pi/7)$ . It is not possible to reduce this requirement to the finding of a single good approximation. The results of a systematic computer search for such approximations are shown in table 3. Numerical verification of these results, using single precision arithmetic (4 or 5 bytes) is possible for values of distance up to about 30 000; to go farther requires the use of multiple precision arithmetic.

**Table 3.** Successive least minima of  $v_7$ .

Distance	Variance	Distance/ $(\pi/2)$
8.3004	0.817	
22.612	0.205	14
78.313	0.111	50
148.33	0.106	94
204.04	5.03 E-2	130
430.69	1.73 E-2	274
713.04	5.03 E-3	454
6 487.4	9.21 E-4	4 130
59 021.1	2.78 E-5	37 574
536 964.2	8.74 E-6	31 842
2 472 116.1	8.01 E-6	1 573 798
2 950 059.2	4.27 E-6	1 878 066
4 885 211.1	1.87 E-7	3 110 022
155 288 469	1.64 E-7	98 859 710
204 618 523	5.70 E-8	130 264 198

The quantity (distance/ $(\pi/2)$ ) is very close to an integer in each case in table 3, and is the common denominator in the three rational approximations to the three cosines.

The data of table 3 are plotted on logarithmic scales in figure 7. The straight line satisfies the equation

$$\text{variance} = 1/\text{distance}.$$

The points lie close to this line: only one point lies below it, but it would be rash to attempt to fit a line to the data: all that can be said is that for  $q = 7$  the least successive variance appears to fall off almost linearly with distance, rather than quadratically as found for  $q = 5$  and  $q = 8$ .

Examination of the data of table 3 has not shown any regularities among successive least minima, other than that all three rational fractions are of the form  $(2j + 1)/(4k + 2)$ : this observation considerably speeded up the search for minima.

The least successive minima appear to fall off linearly with distance, but there is no obvious pattern. We have carried out a computer search for successive least minima

to a distance of  $2 \times 10^8$ : further searching is likely to require excessive amounts of computer time, since there appears to be about one new least minimum per decade.

Extending table 3 to greater values of distance is very time-consuming: the search using FORTRAN on an Archimedes advances at a rate of about  $10^7$  per day: even on a supercomputer the rate would be at best a very few decades higher, and it would be difficult to leave a supercomputer running the program for an entire week, as one can do with a microcomputer.

In an attempt to find some pattern among the convergents to  $\cos(\pi/7)$ ,  $\cos(2\pi/7)$  and  $\cos(3\pi/7)$  we have looked also at the continued fraction convergents of the three cosines separately, to see if there was any tendency for terms with equal denominators to appear. The only finding was that certain numbers appeared as the numerator of one fraction and as the denominator of another (in a cyclic sense), but no pattern was apparent. Note that the three cosine terms are the roots of a cubic equation. The regularity in spacing associated with the earlier quadratic cases does not apply.

## 7. Conclusions

Some of the trajectories generated by the standard map with twist appear to be nearly straight lines even in non-crystallographic cases. The mapping can be derived from a Hamiltonian  $\mathcal{H}$  in the limit of small nonlinearity.

The Hamiltonian  $\mathcal{H}_q$  generates crystallographic tilings of the plane when  $q$  is equal to a crystallographic value (3, 4, 6). For other values of  $q$  a crystallographic tiling is not possible, but in two cases ( $q=5$  and  $q=8$ ) and possibly in a third case ( $q=7$ ) we find straight lines which can approximate energy contours as closely as we please. The cases of  $q=5$  and  $q=8$  are distinguished by the fact that they each involve rational approximations for a single (quadratic) irrational.

The existence of these straight lines along which the variance of the energy is very small explains the strong appearance of 'nearly straight line' trajectories in the standard map with twist.

## Appendix A. The derivation of a Hamiltonian from the standard map with twist

The map  $M_q$  when applied  $q$  times is approximately the identity in the limit  $k \rightarrow 0$ .

The  $q$ th iteration of the map, to first order in  $k$ , is

$$\begin{aligned} x &\rightarrow x + k \sum_{p=0}^{q-1} \cos(2\pi p/q) \sin\{-x \cos(2\pi p/q) + y \sin(2\pi p/q)\} \\ y &\rightarrow y + k \sum_{p=0}^{q-1} \sin(2\pi p/q) \sin\{-x \cos(2\pi p/q) + y \sin(2\pi p/q)\} \end{aligned}$$

so the limiting form of the invariant curves comes from the flow

$$\begin{aligned} \frac{dx}{dt} &= \sum_{p=0}^{q-1} \cos(2\pi p/q) \sin\{-x \cos(2\pi p/q) + y \sin(2\pi p/q)\} = -\frac{\partial \mathcal{H}}{\partial y} \\ \frac{dy}{dt} &= \sum_{p=0}^{q-1} \sin(2\pi p/q) \sin\{-x \cos(2\pi p/q) + y \sin(2\pi p/q)\} = \frac{\partial \mathcal{H}}{\partial x} \end{aligned}$$

where  $\mathcal{H}$  is the Hamiltonian  $\mathcal{H}_q$  defined in equation (2).

**References**

Bak P 1985 *Phys. Rev. B* **32** 5764-72

Chernikov A A, Sagdeev R Z, Usikov D A, Zakharov M Y and Zaslavsky G M 1987a *Nature* **326** 559-65  
— 1987b *Phys. Lett.* **125A** 101-6

Hardy G H and Wright E M 1954 *An Introduction to the Theory of Numbers* (Oxford: Oxford University Press)

Sagdeev R Z, Usikov D A and Zaslavsky G M 1988 *Nonlinear Physics* (New York: Harwood)

Schechtman D, Blech I, Gratiias D and Cahn J W 1984 *Phys. Rev. Lett.* **53** 1951-3